Peer-Reviewed Technical Communication

Station-Keeping Underwater Gliders Using a Predictive Ocean Circulation Model and Applications to SWOT Calibration and Validation

Evan B. Clark, Andrew Branch, Steve Chien, Faiz Mirza, John D. Farrara, Yi Chao, David Fratantoni, David Aragon, Oscar Schofield, Mar M. Flexas, and Andrew Thompson

***Abstract*—Instrumented ocean moorings are the gold standard for gathering *in situ* measurements at a fixed location in the ocean. Because they require installation by a ship and must be secured to the seafloor, moorings are expensive, logistically difficult to deploy and maintain, and are constrained to one location once installed. To circumvent these issues, previous studies have attempted to utilize autonomous underwater gliders as platforms for virtual moorings, but these attempts have yielded comparatively large station-keeping errors due to the difficulty of glider control in dynamic ocean currents. We implemented an adaptive planner using a vehicle motion model and a predictive ocean circulation model to improve station-keeping performance by incorporating anticipated currents into glider control. We demonstrate improved station-keeping performance using our planner in both simulation and in-field deployment results, and report smaller average station-keeping error than the Monterey Bay Aquarium Research Institute's M1 mooring. Finally, we utilize our simulation framework to conduct a feasibility study on using an array of autonomous gliders as virtual moorings to conduct critical calibration and validation (CalVal) for the upcoming National Aeronautics and Space Administration, Surface Water and Ocean Topography (SWOT) Mission, instead of using permanent moorings. We show that this approach carries several advantages and has potential to meet the SWOT CalVal objectives.**

***Index Terms*—Adaptive control, autonomous systems, oceanographic techniques, predictive control, predictive models, unmanned underwater vehicles.**

I. Introduction

MANY of the critical science questions facing the oceanographic community require sustained spatial sampling to not only measure the mean state of the system but also high-frequency changes that can have disproportionately large effects on the physics, biology, and chemistry. This is difficult and cost prohibitive using traditional sampling approaches based on ships or moorings. Ships cannot maintain a sustained spatial presence at sea, and as moorings can maintain an excellent sustained temporal presence in the sea, they are expensive. Fortunately, autonomous underwater vehicles (AUVs) have matured and are becoming reliable tools to collect data for sustained periods of time, filling a critical gap in sampling the ocean [1], [2]. These vehicles have many advantages as they are easier/less expensive to deploy and more versatile once deployed. For example, multiple vehicles can be deployed at a single location or directed to conduct spatial surveys. The challenge is to develop a scalable approach that allows for sustained deployment of multiple vehicles given the significant shoreside human effort required to pilot the fleet of vehicles in the field. For large fleets of gliders operated during large field campaigns, this often requires a dedicated team of AUV "pilots" with the number of personal tied directly to the number of vehicles deployed [3]. For campaigns that utilize many vehicles (tens and even more), the availability and cost of the personnel become the bottleneck and there is a critical need to develop automation and tools to assist in the managing fleets of vehicles.

To overcome this hurdle, the community has focused on developing coupled vehicle and numerical model networks that provide a potentially scalable path forward by allowing for automated command/control [4]–[6]. Developing scalable approaches will be increasingly important given several large planned field efforts. For example, Surface Water and Ocean Topography (SWOT) is a future NASA/CNES mission set to launch in 2021, aimed at better understanding earth's oceans and its terrestrial surface waters. SWOT will conduct a global survey of earth's surface water with unprecedented resolution, allowing scientists to better understand subjects from water supply to oceanic circulation to climate change [7]. A vital aspect of the mission involves calibrating and validating the sensors aboard the satellite using *in situ* measurements acquired by assets in the ocean (CalVal). A conventional approach would require deploying instrumented moorings at specific locations in the overflight path of the satellite, but physical moorings are expensive to deploy and maintain. SWOT's CalVal requirement specified on wave number spectra imposes significant difficulty for an ocean *in situ* observing system. Due to the quickly changing ocean surface topography (timescale of several hours), approximately 20 measuring locations are required to capture the synoptic field to serve as ground truth to satellite measurement taken within tens of seconds [8]. An array of 20 instrumented moorings would be very expensive in the standard of satellite CalVal. As an alternative approach, a dynamically controlled marine vehicle can act as a "virtual mooring" by attempting to station keep in one

Manuscript received March 13, 2018; revised August 14, 2018; accepted December 5, 2018. This work was supported in part by the NASA SWOT project, in part by the JPL Research and Technology Development Program, and in part by the Keck Institute for Space Studies (generously supported by the W. M. Keck Foundation) through the project "Science-driven Autonomous and Heterogeneous Robotic Networks: A Vision for Future Ocean Observation" (http://www.kiss.caltech.edu/new_website/techdev/seafloor/seafloor.html). *(Corresponding author: Evan B. Clark.)*

Associate Editor: R. Bachmayer.

E. B. Clark, S. Chien, F. Mirza, and A. Branch are with the Jet Propulsion Laboratory, California Institute of Technology, Pasadena, CA 91109 USA (e-mail: evan.clark@jpl.nasa.gov; steve.a.chien@jpl.nasa.gov; faiz.mirza@jpl.nasa.gov; andrew.branch@jpl.nasa.gov).

J. D. Farrara, Y. Chao, and D. Fratantoni are with the Remote Sensing Solutions, Monrovia, CA 91016 USA (e-mail: jfarrara@remotesensingsolutions.com; ychao@remotesensingsolutions.com; fratantoni@remotesensingsolutions.com).

D. Aragon and O. Schofield are with the Rutgers University, New Brunswick, NJ 08901 USA (e-mail: dkaragon@marine.rutgers.edu; oscar@marine.rutgers.edu).

A. Thompson and M. M. Flexas are with the California Institute of Technology, Pasadena, CA 91125 USA (e-mail: andrewt@caltech.edu; marf@caltech.edu).

Digital Object Identifier 10.1109/JOE.2018.2886092

location despite the presence of ocean currents [9], and an array of such vehicles could cover the 20 locations required by SWOT.

There are a number of vehicles to consider for the task of station keeping with varying costs and capabilities. These range from inexpensive vertically profiling floats with no horizontal control and deployment times on the order of years [6] to more expensive short-range AUVs with significant control authority—approximately 2.5 m/s horizontally—with deployment times on the order of hours [10] to ships carrying sensor packages lowered on cables. Each platform has its advantages and disadvantages, and ultimately, the best choice of asset type(s) to use will be determined by the scientific question at hand. Underwater autonomous gliders are a promising choice for virtual moorings since they are inexpensive compared to permanent instrumented moorings, capable of being deployed for months at a time, and can travel horizontally at approximately 0.25 m/s.

To enable the virtual mooring array concept for calibrating the SWOT mission, our approach uses a predictive model of ocean circulation and a greedy search algorithm to simulate each vehicle's future motion and select the control action that results in the best station-keeping performance in the presence of dynamic ocean currents. The remainder of this paper is organized as follows: First, we present results of a station-keeping field deployment conducted off the California coast near Monterey Bay using the station-keeping planner as well as baseline (no planner) control. Second, we develop the conceptual framework for conducting simulated station-keeping deployments, compare and contrast the simulation results to results from the field, and use simulations to study the effect of planning model accuracy on station-keeping performance. Third, we use simulations to study the viability of our virtual mooring approach as applied to the SWOT CalVal requirements: station keeping much further off the coast at the location of the SWOT overflight path and for significantly longer durations—and use these results to generate recommendations for SWOT mission planners. Finally, we discuss the next steps needed for further improvement and validation of our method.

A. Related Work

Many literature works exist relating to general path planning of underactuated marine vehicles. Thompson *et al.* [11] use the Regional Ocean Modeling System (ROMS) model with wavefront propagation to control gliders in the presence of currents. Rao and Williams [12] employ rapidly exploring random trees to plan glider paths over long distances. Pereira *et al.* [13] use path planning to prevent gliders from surfacing in dangerous locations. Dahl *et al.* [14] utilize a number of planning algorithms to optimize float coverage across all oceans. Alvarez *et al.* [5] use a genetic algorithm with no ocean model to control a network of floats and gliders. Leonard *et al.* [4] use coordinated feedback control laws to implement cooperative sampling patterns for a heterogeneous fleet of marine assets. Jones and Hollinger [15] use ROMS for planning energy efficient trajectories for an autonomous boat in the presence of uncertainty and limited data.

Some works have been done regarding station keeping with underactuated marine vehicles. Hodges and Fratantoni [9] and Rudnick *et al.* [16] both use gliders as virtual moorings, but they do not use an ocean circulation model to anticipate and counteract ocean currents before each dive although they do generate control sequences. Hodges and Fratantoni [9] achieve an average distance from the mooring location of 2.0 km and Rudnick *et al.* [16] achieve an average distance of 3.6 and 1.8 km in two separate experiments. Troesch *et al.* [6] present an approach for station keeping with vertically profiling floats using ROMS by taking advantage of different current directions at different depths, and investigate this concept in terms of the effect of planning model accuracy and batch versus continuous planning.

The concept of using underwater gliders as virtual moorings for SWOT CalVal has been investigated by Wang *et al.* [8] who conducted a study characterizing CalVal performance using both traditional and virtual moorings in simulation. The simulation found that only traditional moorings are suitable to meet the SWOT mission requirements although virtual moorings implemented with gliders come close. However, the gliders in this simulation did not actively compensate for control disturbances due to currents—they only attempted to dive straight back toward the target and changed their dive path angle from 60° to 30° when the glider-to-target distance crossed a 6-km threshold—so it is likely that their station-keeping performance could be improved with more sophisticated control schemes. Although the simulated gliders did not meet the standards set by the SWOT CalVal requirements, Wang *et al.* [8] acknowledged that there was room for improvement in the glider control scheme and recommended that the virtual mooring concept merits further study and development.

B. Vehicles

Our approach employs two types of vehicles, the Kongsberg seaglider [17] and the Teledyne Webb Research Slocum glider [18]. Both vehicles are similar in function and operate using the same locomotion principle. Each vehicle is equipped with a variable buoyancy engine and wings. Changing the buoyancy of the vehicle negative or positive allows the vehicle to glide up or down in the water column using very little energy, resulting in a "sawtooth" trajectory. This energy efficiency allows the vehicle to operate for months at a time and travel thousands of kilometers on a single battery charge. The Slocum glider and seaglider have nominal through-water speeds of 0.35 and 0.25 m/s while diving, respectively. The Slocum glider may also optionally be equipped with a rear-mounted propeller (thruster) to enable horizontal flight or supplement the glider's velocity through the water during buoyancy-driven dives.

The station-keeping planner algorithm requires a vehicle motion model to compute the trajectory of the vehicle through the water during a simulation. We used a simple geometric vehicle motion model that assumes a fixed through-water speed for both the seaglider and the Slocum glider. The vehicle motion model for the seaglider was given by

$$s_x = 0.25 \cos(\alpha) \tag{1}$$

$$s_y = 0.25 \sin(\alpha) \tag{2}$$

where α is the dive path angle, and s_x and s_y are the horizontal and vertical components of the through-water speed of the glider, respectively, in meters per second. The Slocum glider may optionally spin a rear-mounted thruster to increase its through-water speed, so the vehicle motion model for the Slocum glider was modified to

$$s_x(p_T) = (0.35 + s_e(p_T)) \cos(\alpha) \tag{3}$$

$$s_y(p_T) = (0.35 + s_e(p_T)) \sin(\alpha) \tag{4}$$

$$s_e(p_T) = 0.0951 p_T \tag{5}$$

where s_e is the extra through-water speed contributed to the Slocum glider by the thruster, and p_T is the power set point of the thruster, in watts. The value of 0.0951 in (5) was determined empirically through field testing by the Teledyne Webb Research [19].

While more sophisticated vehicle motion models, such as in [20]–[22], could be employed to simulate the vehicle dynamics, for purposes of our planner, we choose to simulate the vehicle as a point object

and treat all dive trajectories as idealized geometry for simplicity. It is likely that a more accurate vehicle motion model could further improve station-keeping performance, but as a first pass, the planner only needs to better estimate vehicle trajectories in the presence of currents than the naive baseline approach without the planner. Using a more accurate vehicle motion model is a promising avenue for future improvement to the planner.

The Spray glider is a similar type of buoyancy-driven glider [23]. We did not include it in our study because we did not have a Spray glider available for physical deployments and it has very similar performance specifications on paper to the seaglider, so we did not feel that it would add significant value to the simulation results.

C. Ocean Circulation Models

Our approach requires an ocean circulation model with predicted currents at sufficient spatial and temporal resolutions (on the order of kilometers in the horizontal direction, meters in the vertical direction, and hours in the time dimension) and a sufficient timespan for the duration of the mission. Some widely used ocean models that fit this criteria include the ROMS [24], the Harvard Ocean Prediction System (HOPS) [25], the Princeton Ocean Model (POM) [26], the Hybrid Coordinate Ocean Model (HYCOM) [27], the Massachusetts Institute of Technology General Ocean Circulation Model (MITgcm) [28], and the Nucleus for European Modelling Ocean Engine [29]. We used the ROMS. Within Monterey Bay, the horizontal resolution of the ROMS model we used was 300 m $\times$ 300 m grid spacing, and outside it was 3 km $\times$ 3 km. The depth resolution for the 300-m model was 24 depths ranging from 0 to 1200 m with nonuniform spacing. The depth resolution for the 3-km model was 14 depths ranging from 0 to 1000 m with non uniform spacing. Atmospheric forcing for the ROMS model is derived from hourly operational forecasts of the NCEP 5-km North American Model [30]. Tidal forcing is derived from the TPXO.6 global barotropic tidal model [31]. Other inputs are archiving, validation and interpretation of satellite oceanographic (AVISO) sea surface height data, advanced very high resolution radiometer (AVHRR) and moderate resolution imaging spectroradiometer (MODIS) sea surface temperature, high frequency (HF) radar surface current data, and instrumented measurements from the Monterey Bay Aquarium Research Institute (MBARI) M1 mooring and ships. Every day by 1200 coordinated universal time (UTC), ROMS produces a two-day forecast of ocean conditions using a nowcast at 0300 UTC incorporating the latest data as its initial state. Each forecast consists of 48 time slices at 1-h intervals. For purposes of our simulations lasting longer than one day, we use the prediction given by the most recent ROMS forecast. More information about the ROMS model can be found in [32].

D. Station-Keeping Algorithm

Present approaches to station keeping with gliders either do not take control disturbances due to ocean currents into account (effectively assuming that there are zero ocean currents) or use an estimate of ocean currents built up from the error between the vehicle's expected and actual surfacing locations on recent previous dives. Our station-keeping algorithm uses a predictive model of ocean currents and a vehicle motion model to anticipate the control disturbances that will be observed by a glider on its next dive, and then select a control scheme that will compensate for those disturbances during the dive. It should be noted that to improve station-keeping performance, the predictive ocean current model and the vehicle motion model do not have to be perfect, they only need to enable the planner to better estimate vehicle trajectories in the presence of currents than the (implicit) assumptions of the baseline approach.

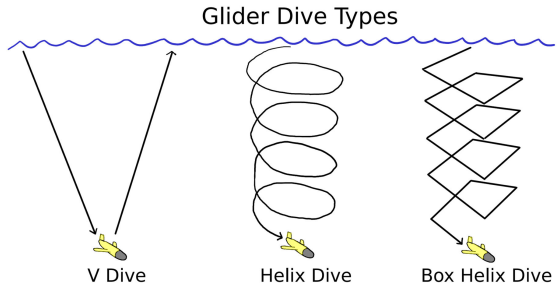

Fig. 1. Visualization of dive types available to each vehicle. For the deployments and simulations discussed in this paper, seagliders may perform V dives and helix dives and Slocum gliders may perform V dives and box helix dives. Controllable parameters for V dive are dive path angle, heading, and depth. Controllable parameters for helix dive are dive path angle, depth, and helix radius. Controllable parameters for box helix dive are dive path angle, depth, box center and side length.

The station-keeping planner requires a vehicle motion model, a predictive model of ocean circulation, and a station-keeping target location as inputs. The goal is to minimize the average station-keeping error, where error is defined as the distance between the glider surfacing position after each dive and the target station-keeping location.

We employ a continuous, greedy planning algorithm to generate the required control sequences for the glider. At each surfacing, the glider may pick from a variety of dive types to execute next, a "V dive," a "helix dive," or a "box helix dive," where a dive is defined as the set of control actions between two surfacings, i.e., both descent and ascent through the water. The various dive types are detailed in Fig. 1 and each is defined by a number of parameters, including dive heading. Generally speaking, the V dive is best for moving quickly back to the target location when far away, since it covers larger horizontal distances, and the helix and box helix dive are better for staying tight around the target when the currents are weak. Additionally shorter (in time) dives may assist station-keeping performance because they allow for a faster control feedback cycle in terms of opportunity to recommand the vehicle back toward the station-keeping target. For the purposes of this paper, only seagliders may use the helix dive and only Slocum gliders may use the box helix dive for firmware reasons. Optionally, Slocum gliders may also spin a thruster mounted at the rear of the vehicle at variety of speeds that each add a constant offset to the vehicle's through-water velocity. For each dive, the station-keeping planner discretizes a search angle centered around the bearing of the station-keeping target waypoint into N discrete headings. Then, it simulates every possible combinatorial set of dive parameters for dives using these headings using the vehicle motion model and the predictive ocean circulation model. The simulation is conducted by applying the selected dive parameters to the vehicle motion model to compute the vehicle velocity vector. At specified time intervals, the currents affecting the glider are updated based on the predictive ocean model by linearly interpolating the current velocity vector based on the glider latitude, longitude, depth, and time in the simulation. This velocity vector is added to the velocity vector computed from the vehicle motion model, and the combined vector is used to compute the location of the glider at the next time step. This is repeated until the glider completes its dive by surfacing. The algorithm then selects the dive parameter combination that results in surfacing closest to the station-keeping target location. Finally, the planner sends the dive command with the best parameters to the glider, which executes the command in the ocean. A visualization of the algorithm is shown in Fig. 2.

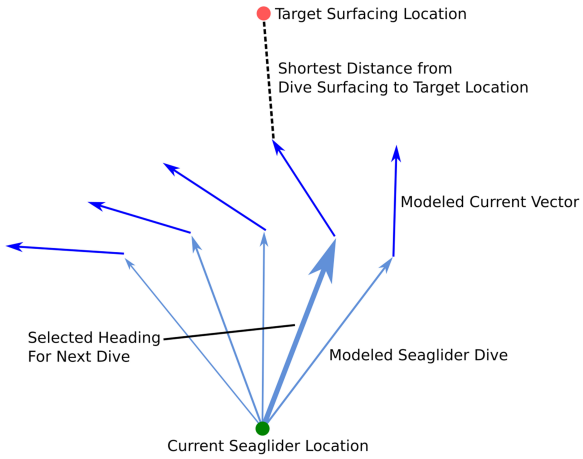

Fig. 2. Visualization of the adaptive station-keeping algorithm in the presence of dynamic ocean currents. Before each dive, the planner simulates the trajectory for the next dive using the vehicle motion model and the predictive ocean circulation model. The dive parameters are chosen that results in the simulated dive that surfaces closest to the station-keeping target waypoint, then sent to the vehicle to be executed in the ocean.

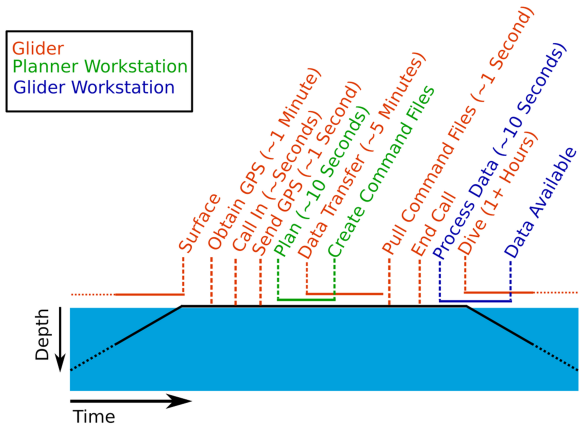

Fig. 3. Data flow timeline for one surfacing of the glider. The planner server may be run on a dedicated computer or on the existing infrastructure that processes incoming glider data during a normal glider deployment, in which case the planner workstation and glider workstation are the same computer.

The station-keeping algorithm is run off-board the vehicle, on a shore (or ship) based station-keeping planner server, which may be implemented with a standard Internet-connected laptop. The predictive ocean circulation model, vehicle motion model, and planner software are stored on the planner server. Communication with the vehicle is established via Iridium satellite link when the vehicle surfaces. At each surfacing, the planner receives the current GPS location of the glider, computes the next dive command based on this new location and the state of the predictive ocean current model, then sends the next dive command back to the glider. All of this occurs on one surfacing, allowing for a closed-loop control. The planner conservatively requires 15 s to generate a plan from when the glider first connects to the shore-based control workstation, which includes retrieving the vehicle location and loading the required model data. The planner workstation does these computations in parallel while the glider is sending back its other science data, so the only time cost incurred by the glider is to downlink the plan, which takes about 1 s (see Fig. 3). The glider is nominally on the surface for approximately 5 min total, depending on the amount of other science data it is sending to shore and the quality of the satellite data link, thus

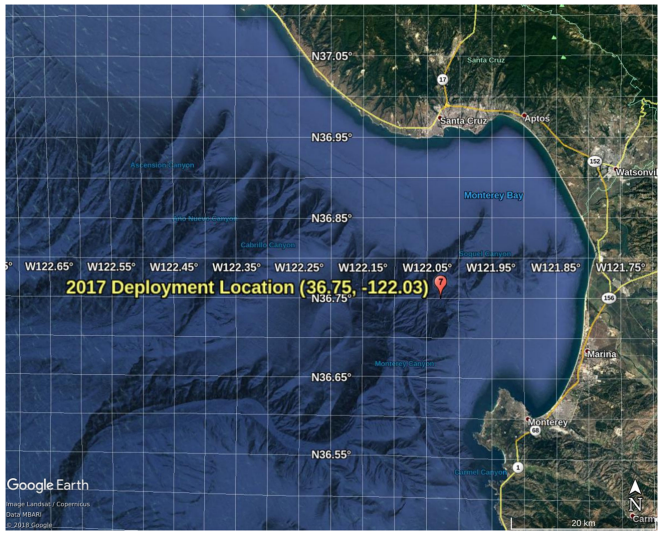

Fig. 4. Map of operations area for 2017 deployment.

incorporation of the planner does not add significant time spent at the surface.

The station-keeping algorithm is greedy and only looks one dive ahead. Although it would be easy to extend the planner to look more than one dive ahead, we found that doing so does not significantly improve performance because the planner has a chance to revise the plan at each surfacing. The latest plan will always be best for the next dive because the most information is available, so any plans made further in the past get overwritten. This is analogous to if you were making a decision to carry an umbrella due to possible rain today given today's weather forecast versus a three-day old weather forecast for today. You would always listen to today's forecast because it incorporates the latest information.

During (nonsimulated) deployments, temperature, salinity, and depth-averaged current velocity data measured by the vehicle's sensors are assimilated back into the predictive current model inputs to improve future predictions by providing *in situ* forcing. In our case, because ROMS forecasts are only produced once a day, in practice, this means that the feedback does not show up for the planner until the next forecast is published the following day. Such feedback is not assimilated during simulated deployments because those run faster than real time and it would be impractical to recompute the ROMS model to incorporate feedback, and also it is unclear what such feedback would mean in the context of simulated ocean environments.

II. Station-Keeping Deployment

To test the station-keeping algorithm on real vehicles in an ocean environment, we conducted a station-keeping deployment from June 23rd to July 24th, 2017 near the M1 mooring operated by the MBARI (36.75° N, 122.03° W). The deployment location is shown in Fig. 4. We utilized two types of vehicles, the Slocum glider and the Kongsberg seaglider, and conducted station-keeping experiments using both planner control and baseline control (without the planner). The Slocum glider did not use its thruster for this experiment. The dive depth was fixed at 500 m for all experiments, because this is likely what would be used for a future glider-based SWOT virtual mooring CalVal campaign. The depth of 500 m was chosen as a balance between measuring as much stratified ocean as possible (to reduce error in estimating dynamic sea surface height) while also maximizing the profiling rate (to reduce

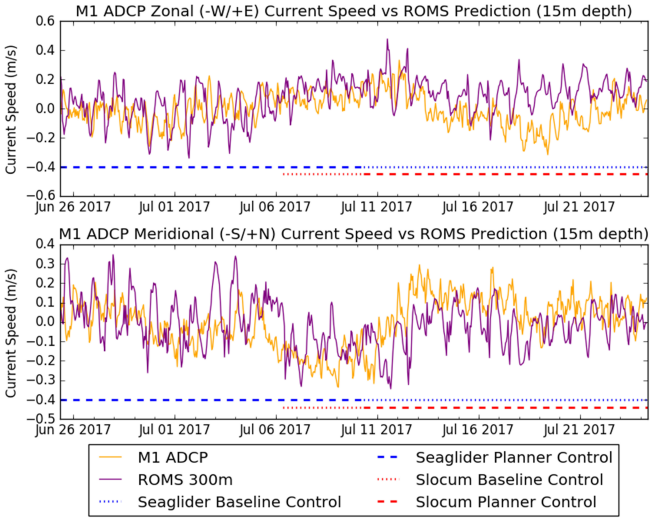

Fig. 5. M1 ADCP measured current speed at 15-m depth for the duration of the 2017 glider station-keeping deployment. Dotted and dashed lines show the timeline of the type of control used by each vehicle (planner or baseline control).

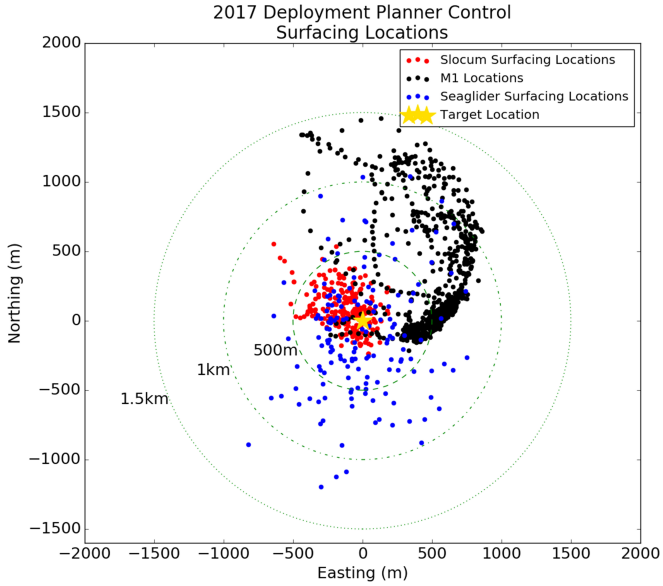

Fig. 6. Surfacing locations for the seaglider and Slocum glider under planner control during the 2017 deployment. GPS locations for the MBARI M1 mooring are also shown. The station-keeping waypoint for each asset is co-located to a shared origin for ease of visualization.

temporal smearing). The planner was allowed to select the best dive type (V dive or helix dive for seaglider and V dive or box helix dive for Slocum glider), dive path angle and heading for V dives, and dive path angle for helix dives and box helix dives, centered at the current location. Helix dives had a fixed angular turn rate set in firmware to 1 deg/s, causing approximately 8-m radius helixes nominally. Due to a mix-up in the field, box helix dives had a fixed side length of 100 m under planner control and 150 m under baseline control. The box sides were oriented along the cardinal directions. Vehicle-measured temperature, salinity, and depth-averaged current velocities were assimilated (fed back) into the predictive ocean current model as part of the cycle preparing for the next day's forecast.

Fig. 5 shows the 15-m depth current speeds measured by the acoustic Doppler current profiler (ADCP) mounted on the MBARI M1 mooring for the duration of the deployment. Only 15-m depth is shown for visual simplicity because the currents were generally fast near the surface, so this is meant to represent an approximate upper bound on current speed experienced by the vehicles. Over the course of the deployment, the 15-m depth current magnitudes at M1 ranged from 0.004 to 0.366 m/s with an average magnitude of 0.150 m/s. For the seaglider, the average magnitude was 0.159 m/s during the baseline control phase, and 0.141 m/s during the planner control phase. For the Slocum glider, the average magnitude was 0.212 m/s during the baseline control phase and 0.159 m/s during the planner control phase. The average current magnitude was well under the nominal through-water speed of both the seaglider and Slocum during all phases of the deployment.

Several baseline control experiments were conducted where the vehicle attempted to station keep without use of the planner. In the case of the seaglider, this meant that the vehicle performed fixed 30° V dives aimed back toward the station-keeping waypoint with current compensation implemented by the proprietary onboard Kalman filter that applies current compensation control based on errors between expected and actual surfacing locations on recent previous dives. In the case of the Slocum glider, the vehicle performed naive box helix dives centered at the station-keeping target location. The dive path angle was fixed to 30° in all baseline experiments.

Station-keeping experiments were also conducted using the planner using a 300-m ROMS model. The amount that the planner can improve station-keeping performance is highly dependent on the accuracy of the current model with respect to the real currents experienced by the vehicle. In addition to the 15-m depth currents measured by the M1 ADCP, Fig. 5 also shows the 15-m depth currents predicted by ROMS. The error vector magnitude e between the current measured by the M1 ADCP and the current predicted by the ROMS model at a given time t is given by the following equation:

$$e_t = \sqrt{(u_{M1t} - u_{\mathrm{ROMS}_t})^2 + (v_{M1t} - v_{\mathrm{ROMS}t})^2}. \quad (6)$$

Then, the root mean square (RMS) error of the ROMS 15-m depth predicted currents with respect to the measurements made by M1 is given by

$$\mathrm{RMSE} = \sqrt{\sum\nolimits_t e_t^2 / |t|}. \quad (7)$$

The RMS error between ROMS and the M1 measurements was 0.234 m/s over the course of the whole deployment. For the seaglider, the error was 0.249 m/s over the baseline control phase and 0.218 m/s over the planner control phase. For the Slocum, the error was 0.185 m/s over the baseline control phase and 0.249 m/s over the planner control phase. Although the errors of the ROMS model were relatively large over the course of the deployment, it is important to remember that in order for the planner to improve station-keeping performance, the predictive current model does not need to be a perfect representation of the true ocean state, only a *better* model than the one that is implicitly used if the planner is not employed (Kalman filter based on previous surfacing error for seagliders or zero current model for Slocums).

Fig. 6 shows the surfacing locations of the vehicles under planner control during the deployment. The location of the M1 mooring during the same time period is also shown. M1 is anchored to the seafloor on a long tether, but does not stay directly above the anchor because it drifts according to the currents until the end of its tether is reached. The axes have been converted into meters northing and easting from the station-keeping waypoint to co-locate the plots on the same origin, although the vehicles did not station keep at the exact same location

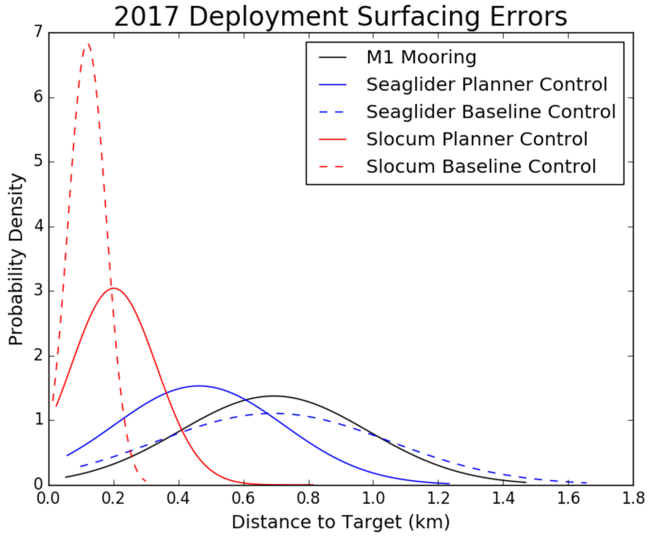

Fig. 7. Estimated probability density function for surfacing error for the seaglider and Slocum glider under both planner and baseline control during the 2017 deployment. The station-keeping error of the MBARI M1 mooring is also shown.

to prevent collisions. Fig. 7 shows the estimated probability density function of surfacing error for each vehicle under both planner and baseline control, as well as for the M1 mooring.

The seaglider performed better under planner control than baseline control, with a station-keeping error of 0.692 km for the period from July 10–23 under baseline control and 0.464 km for the period from June 25 to July 10 under planner control—a 49% reduction in station-keeping error. To attribute this performance gain to the planner, we must discount two other possibilities: first, that the current regime was significantly easier during the planner control phase, and second, whether use of the planner just opened up another dive option that was used exclusively (and thus the same performance gain could be achieved by just statically choosing this option if it was known ahead of time) or planner was actually adaptively making different choices according to the needs of the situation. Addressing the first possibility, current speeds in the M1 area were similar during the baseline and planning control phases, with an average magnitude of 0.159 m/s over the baseline control phase and 0.141 m/s over the planner control phase, both well under the glider's through-water operating speed. Although the average current speed was slightly slower during the planner control phase—0.018 m/s or 12.8% slower—It is unlikely that such a small current difference could account for the 49% reduction in station-keeping error observed. Addressing the second possibility, Fig. 8 shows a histogram of the different dive parameters chosen by the seaglider planner over the course of the planner control phase. The planner did not exclusively settle on one dive option, but rather chose a variety of dives based on the situation, likely using the helix dives when the seaglider was close to the station-keeping target because helix dives have less overshoot, and using V dives with progressively shallower angles, the further it was from the target, as V dives are better at covering large horizontal distances. Thus, as designed, the planner anticipated control disturbances due to currents and adaptively responded to the operational situation at hand, significantly improving the station-keeping performance of the seaglider and reducing the average station-keeping error by 49%.

It should also be noted that the planner was able to improve station-keeping performance even though the RMS error of the ROMS model with respect to the M1 measured currents was relatively high, at 0.218 m/s over the seaglider planner control phase. This is a demonstration of how the ocean current model used by the planner does not need to be perfect to improve station-keeping performance, it just needs to be *better* than the (implicit) assumptions made by the baseline control scheme.

The Slocum glider was able to station keep extremely precise under both planner and baseline control, but actually performed better under baseline control than planner control, with an average surfacing error of 0.120 km for the period from July 6–10 under baseline control and 0.201 km over the period of July 10–24 under planner control, or about 67.5% worse under planner control.

There are three plausible explanations for this. The first possibility is that the current regime was easier during the baseline control phase. However, the average current speed was actually faster during the baseline control phase than the planner control phase, at 0.212 and 0.159 m/s, respectively, so this does not explain the discrepancy. The second explanation is that the currents predicted by the planning model were not representative of the true ocean state, so utilizing them for planning did not help, or in fact hurt, station-keeping performance. This explanation may have some merits—the ROMS predictions were less accurate over the course of the Slocum planning phase than that of the seaglider planning phase, with RMS errors of 0.246 and 0.218 m/s, respectively, a difference of about 11%. It is hard to know exactly the extent to which the increase in planning model error could have adversely affected station-keeping performance (although this phenomenon is studied in simulation in Section III), but it is unlikely that the relatively small increase in planning model error could cause the 67.5% increase in station-keeping error. The third explanation is the one best upheld by the evidence: the Slocum's faster speed and the relatively weak currents during the deployment (very rarely greater than the Slocum's through-water operational speed of 0.35 m/s) allowed station-keeping performance to be so good that the planner could not improve it further, and the observed results are mostly noise. Examining the frequency of dive choices in Fig. 7 supports this hypothesis: the planner chose only to execute box helix dives and never V dives, presumably because the vehicle never moved far enough from the target to justify a V dive. Although the planner did choose slightly different dive angles for some of the box helix dives, this would have had relatively little effect on the end result of the dive (it just would have taken more or less time to complete). Thus, the planner was in essence of executing the same control scheme as followed during the baseline control phase, so the planner contributed little to station keeping for better or for worse, and any observed difference was mostly noise.

The M1 mooring achieved an average station-keeping error of 0.694 km from its nominal anchoring position over the period June 24 to July 10, greater than both the seaglider and the Slocum under planner control.

The 2017 deployment successfully demonstrated usage of the station-keeping planner on two different vehicles in a real ocean environment. The planner improved station-keeping performance on the seaglider but not on the faster Slocum glider. It is likely that the planner helped the seaglider but not the Slocum because the planner can only accrue noteworthy benefits to station keeping if the current regime provides a significant but surmountable amount of antagonism to the vehicle's intended control. In this case, the station-keeping environment was not challenging for the Slocum, so the Slocum could station keep very precisely without use of the planner, and the planner could not improve it further. Overall, both vehicles were able to achieve smaller average station-keeping error using the planner than the MBARI M1 mooring fixed to the seafloor, and achieved better performance than the 2.0-km results achieved by Hodges and Fratantoni [9] and the 1.8 and 3.6-km results achieved by Rudnick [16] in two separate experiments.

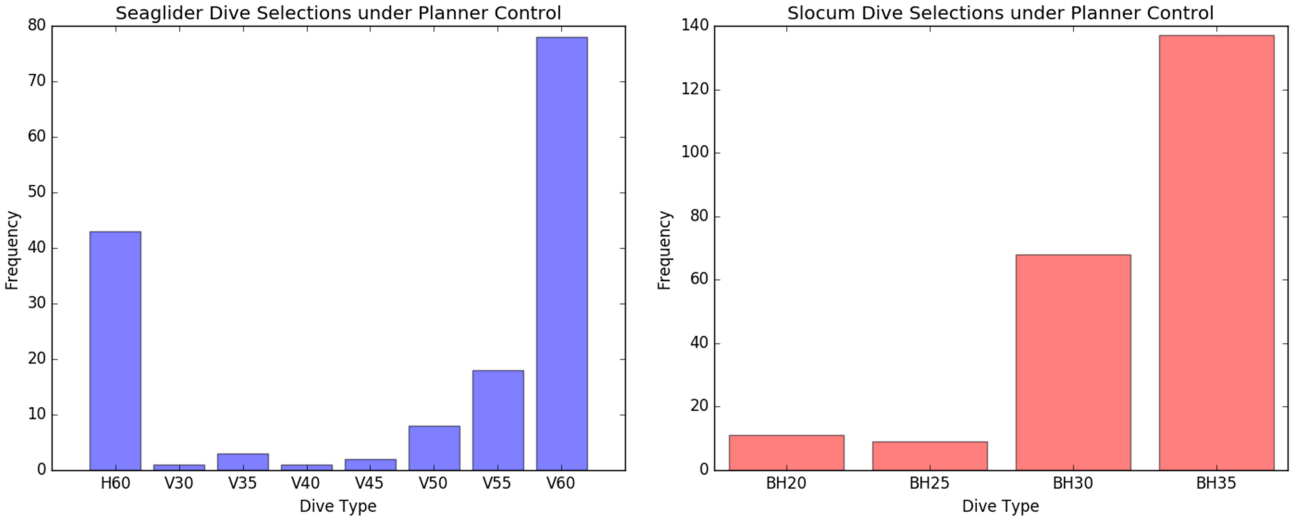

Fig. 8. Frequency of dive selections for the seaglider (left) and Slocum glider (right) during the planner control phase of their deployment. In the *x*-axis labels, letters signify dive type (H: helix dive, V: V dive, and BH: box helix dive) and numbers signify dive path angle in degrees.

III. Station-Keeping Simulations

Ocean deployments are expensive and time consuming, so we developed a simulation framework to allow us to conduct virtual deployments without going into the field. The virtual deployment simulation operates on the same principle as the planner simulation—it applies the currents from the predictive ocean circulation model to the vehicle motion model—except with one more layer of simulation. The planner conducts planning on one predictive ocean circulation model (known as the "planning model"), then the simulation is executed on a different ocean circulation model (known as the "nature model"). The two different models allow us to simulate the fact that in the field the planning model will never truly replicate the real ocean conditions, so there will always be some disparity in what the vehicle believes it will encounter on its next dive versus what it actually does. Furthermore, by varying the difference between the planning model and the nature model, we can directly study how planning model accuracy affects station-keeping performance. To study the effect of planning model accuracy, we generated a nature model, on which the simulation was executed, and a set of planning models where the planner conducted planning. Each planning model was "degraded" by a discrete amount to create a disparity between the nature model and the planning model. The degradation must be representative of how the planning model differs from the ocean in a real deployment, so not just any method (e.g., adding random noise) could be used. To degrade the planning model in a representative way, we used the following approach: the nature model was an archived nowcast ROMS model for a given day that integrated the most up-to-date model predictions and *in situ* data available on that day. The planning models were archived forecasts for that day that had been predicted further in the past. This is analogous to how one would expect the weather forecast for tomorrow to be more accurate than the weather forecast for tomorrow as predicted one week ago.

A. Simulations at M1

The first simulation experiment we conducted aimed to investigate how planning model accuracy effects station-keeping performance. For this experiment, we used an archived nowcast ROMS 300-m model as the nature model, and archived ROMS 300-m forecast models with 2, 4, 6, 8, 10, 14, and 20 days of advance prediction as degraded planning models. We conducted the station-keeping simulation at the location of the MBARI M1 mooring to have some comparison with *in situ* currents measured by the mooring and also to be able to make rough parallels to our 2017 field campaign. However, 2017 300-m ROMS degraded models were not available for our use, so we ran the simulations over the same dates in 2016 to minimize the effects of seasonality on the currents.

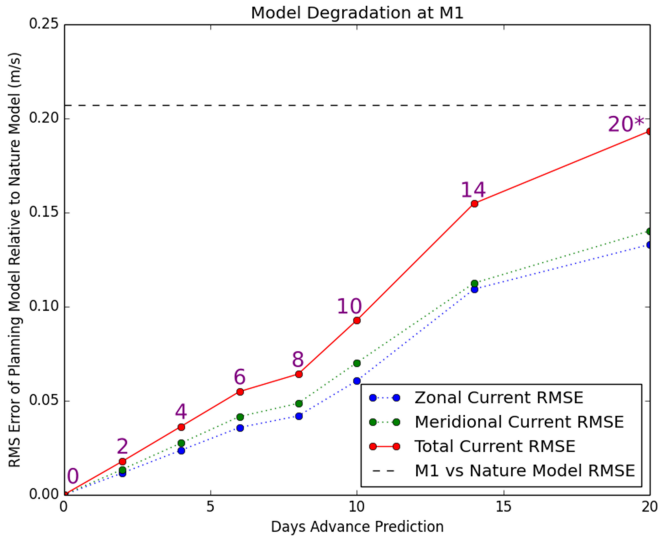

Fig. 9. Planning model RMS error with respect to nature model versus planning model degradation at M1. RMS error was calculated for a 10-km side length square centered around M1 down to 500 m. The period of calculation was July 1st to August 31, 2016. The RMS error of 0.207 m/s between the nature model and the M1 15-m depth currents over the same time period is shown as a horizontal dashed line for reference.

Fig. 9 shows the RMS error of the planning model compared to the nature model for 0–20 days of degradation. The RMS error was computed by differencing all corresponding cells in the planning and nature models in a 10-km side length square centered around M1 down to 500-m depth for a period from July 1 to August 31, 2016. We chose this two-month time period to be long enough to get a representative average error between the models, and also to contain the same dates as the 2017 deployment for running comparative simulations. The error

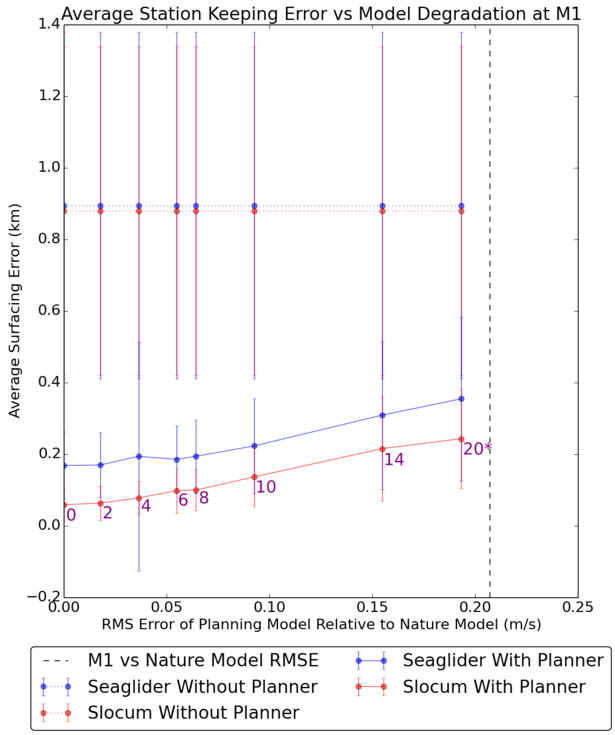

Fig. 10. Average simulated surfacing error versus planning model RMS error at M1. Error bars represent one standard deviation in surfacing error. Purple numbers represent the number of days of degradation for each planning model. The station-keeping simulation period was July 10th–24th, 2016. As in Fig. 9, the corresponding RMS error between the nature model and the M1 measured currents is shown as a dashed line (this time vertical) and most closely corresponds to the error of the 20-day degraded model.

vector magnitude e between the current predicted by the nature model and the planning model for a given time t, latitude lat, longitude lon, and depth d is given in (8) shown at the bottom of this page, where u is the zonal current speed and v is the meridional current speed of the appropriate cell in the two models. Then, the RMS error between the two models is given by

$$\mathrm{RMSE} = \sqrt{\frac{\sum_{t,\mathrm{lat},\mathrm{lon},d} e^2_{t,\mathrm{lat},\mathrm{lon},d}}{|t|\,|\mathrm{lat}|\,|\mathrm{lon}|\,|d|}}. \tag{9}$$

The RMS error of the planning model increases roughly linearly with the number of days of degradation, meaning that the planning model increasingly diverges from nature model as desired.

After acquiring degraded planning models in this way, separate independent simulated deployments were planned using the degraded planning models but executed on the same nature model, and the station-keeping errors of the resulting simulations were compared. The period of simulation for all models was July 10th–24th, 2016 to match the 2017 Slocum planner deployments (2017 300-m ROMS degraded models were not available for our use). Fig. 10 shows the average station-keeping error of each simulation versus the planning model RMS error. In all cases, the planner improved the station-keeping performance of the vehicles by several hundred meters. We can see that for both the seaglider and the Slocum, the average station-keeping error increases as the planning model becomes more degraded, increasing by several hundred meters across the 0–20 days of degradation. This is in line with our expectations—the more accurate the current model available to the planner is, the more the planner can improve station keeping. The planning model accuracy has no effect on the baseline control scheme because that does not take the planning model into account.

Next, we compare the results of our simulation framework to the results we obtained from the 2017 field deployment. This comparison should be taken with a grain of salt because the simulation was calculated for July 10–24, 2016 but the (Slocum) deployment was conducted July 10–24, 2017, and the simulation was planned on an artificially degraded planning model and executed on the nature model, whereas the deployment was planned on the nature model and executed on the real ocean. However, the metric that actually matters for the accuracy of the simulation results is not the accuracy of the nature model itself, but that the error between the planning model and the nature model was similar to the error between the nature model and the true ocean currents. So as long as these errors were similar, the simulation should produce similar results to a real world deployment in terms of station-keeping performance.

Using (7), the RMS error of the 15-m depth currents predicted by the nature model compared to truth M1 measurements over July 1st to August 31, 2016 was 0.207 m/s. This is drawn as a horizontal dotted gray line in Fig. 9 and a vertical gray line in Fig. 10, and corresponds most closely to the error of the 20-day degraded planning model, which has an RMS error of 0.193 m/s compared to the nature model using (9). Therefore, the simulation using the 20-day degraded model as the planning model is the simulation whose planning model error most closely represents the true experience of the vehicles during the 2017 deployment. The 20-day degraded simulation produced seaglider planner average station-keeping error of 0.355 km and a Slocum planner average station-keeping error of 0.243 km. This is quite close to the average station-keeping errors of 0.464 km for the seaglider and 0.201 km for the Slocum observed in the 2017 deployment, showing that the simulation framework can provide reasonable proxy results to an *in situ* deployment. These results are similar enough to the results from the real deployment to merit further simulation study of the virtual moorings concept out at the SWOT crossover area, where we cannot (easily) perform large-scale *in situ* deployment experiments.

B. Simulations at SWOT Crossover Segments

Next, we conducted simulations at locations important for SWOT CalVal to assess the feasibility of the glider-based virtual mooring concept as an alternative to installing instrumented moorings. The SWOT satellite will carry a Ka-band radar interferometer designed to precisely measure water topography along dual 50-km swaths directly underneath the satellite's flight path, with a 20-km gap centered on the nadir track [33]. To effectively utilize the instruments aboard SWOT, calibration and validation must be performed after launch using *in situ* data collected contemporaneously with remote observations from a SWOT overflight. To maximize the value of the *in situ* data, it should be collected near an intersection of ascending and descending SWOT orbital tracks, furthermore known as a "crossover location." For logistical reasons, the most likely crossover location is located about 420 km off the California coast at (125.40° W, 35.55° N), and is known as the SWOT crossover C-Site. At any crossover location, the overlap of the

$$e_{t,\mathrm{lat},\mathrm{lon},d} = \sqrt{\left(u_{M1_{t,\mathrm{lat},\mathrm{lon},d}} - u_{\mathrm{ROMS}_{t,\mathrm{lat},\mathrm{lon},d}}\right)^2 + \left(v_{M1_{t,\mathrm{lat},\mathrm{lon},d}} - v_{\mathrm{ROMS}_{t,\mathrm{lat},\mathrm{lon},d}}\right)^2}. \tag{8}$$

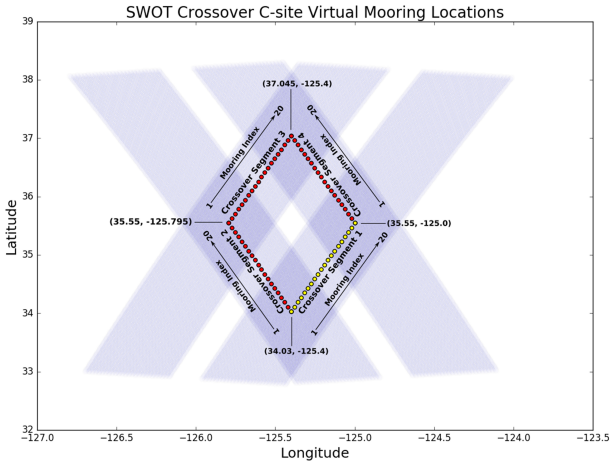

Fig. 11. Operations map for SWOT CalVal C-site crossover locations. Light blue bands show radar swaths for ascending and descending orbits. Dots show proposed virtual mooring locations. Each leg of the diamond represents one virtual mooring array (crossover segment) with locations chosen to maximize overlap between SWOT remote sensing observations and *in situ* mooring measurements. Twenty moorings are placed evenly along the crossover segment (7.5-km spacing). Crossover segment 1 (yellow) was chosen for further study in simulation.

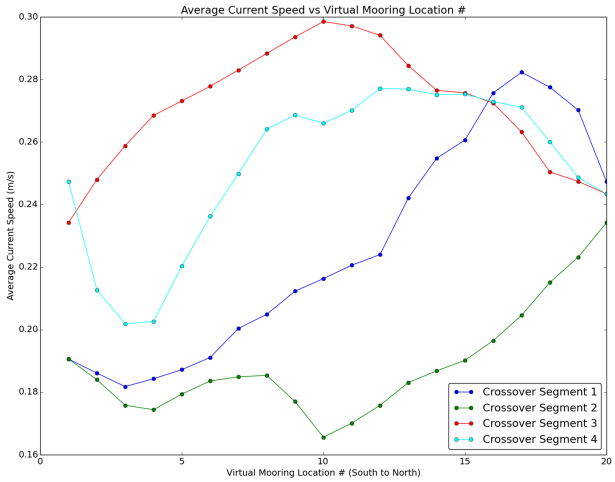

Fig. 12. Effect of virtual mooring location on 500-m depth-averaged current speed for the period July 1, 2017 to September 30, 2017. Virtual moorings are indexed south to north for their respective crossover segment (see Fig. 11).

dual radar swaths from each orbital track forms a diamond shape. To maximize spatial overlap of remote and *in situ* data, the most valuable place to collect data is centered along-track one of the radar swaths and across-track the other two radar swaths from the opposing orbit. This geometry creates four segments of interest, furthermore known as "crossover segments" 1–4. The science requirements specified by the SWOT mission nominally require 20 evenly spaced moorings (7.5-km spacing) along one of the crossover segments to acquire data continuously for 90 days and achieve an average station-keeping error of less than 1.0 km for the duration of the deployment to achieve CalVal [8]. A map of the crossover segments and the candidate virtual mooring locations is shown in Fig. 11. To study the feasibility of the virtual mooring concept for SWOT, we conducted 90-day station-keeping simulations at the 20 candidate mooring locations of crossover segment 1 for the period July 1, 2017 to September 30, 2017.

For this experiment, we used the 3-km California coast configuration of ROMS. As always, the reliability of our simulation is bounded by the accuracy of the ROMS ocean current predictions with respect to reality at the site of the simulation. Because we have no *in situ* data available at the C-site, this accuracy is unknown. However, Chao *et al.* [32] performed validation of depth-averaged currents for this ROMS configuration using data from Spray gliders performing long transects off the California coast. They found that ROMS qualitatively reproduces the flow patterns associated with major current systems such as the California Current and California Undercurrent/Davidson Current, as well as their seasonal variations. They also found that there is tendency for the predicted ROMS currents to be stronger that those observed *in situ*, which would imply that our simulations may underestimate station-keeping performance.

First, we wanted to get a sense of the relative difficulty of station keeping at each virtual mooring location in case one crossover segment was more favorable for operations than the others. Fig. 12 shows the simulated 500-m depth-averaged current speed measured in ROMS over the duration of the simulation. The depth of 500 m was chosen for the same reasons as in the 2017 deployment. We can see that generally speaking, currents get stronger for virtual mooring locations further north, suggesting that station keeping would be more difficult in those locations too. The average current speed data also show that some virtual mooring locations are significantly more difficult than others, for example, virtual mooring location 10 for crossover segment 3 experiences almost double the average current speed than virtual mooring location 10 in crossover segment 2. Overall, crossover segment 2 is the most favorable for station keeping and crossover segment 3 is the least favorable for station keeping for the period of simulation.

We chose to simulate the SWOT CalVal virtual mooring array on crossover segment 1 because it represented the best diversity of station-keeping difficulty in terms of 500-m depth-averaged current speed, covering almost the full range of difficulty observed in the other crossover segments. This segment is also the same segment that was studied in [8]. Fig. 13 shows the average station-keeping error for crossover segment 1 for both seagliders and Slocums with no model degradation (planning model = nature model). The simulations were conducted with baseline control, regular planner control, and also extended planner control where the Slocum gliders had a simulated rear-mounted thruster that could be spun at various speeds to increase the vehicle's velocity through the water at the cost of additional energy expenditure. In the case of the thruster using simulations, the planner was allowed to select the set point of the thruster for each dive, with one group of set points available within a 3-km watch circle radius of the station-keeping waypoint (0–3 W, in increments of 1 W) and an expanded set allowed outside the 3-km radius (0–8 W, in increments of 1 W).

The Slocum gliders with thrusters were able to station keep well under the 1-km target threshold for all virtual mooring locations, with station-keeping errors of 0.061–0.113 km. The Slocum gliders without thrusters could successfully station keep at virtual mooring locations 1–11, but could not maintain the 1-km average error threshold further north than that, as the stronger currents blew the vehicles off station. Having less control authority, the seagliders fared worse and were only able to station keep within the 1-km average error boundary at a handful of locations, and only when using the planner. Generally, as expected, we observed that the larger the 500-m depth-averaged current speed for a virtual mooring location, the more trouble vehicles had for station keeping at that location, sometimes being blown off course tens to hundreds of kilometers in the most extreme cases. Only the Slocum glider using both planner and thruster was able to maintain average station keeping under the 1-km error boundary for all virtual mooring

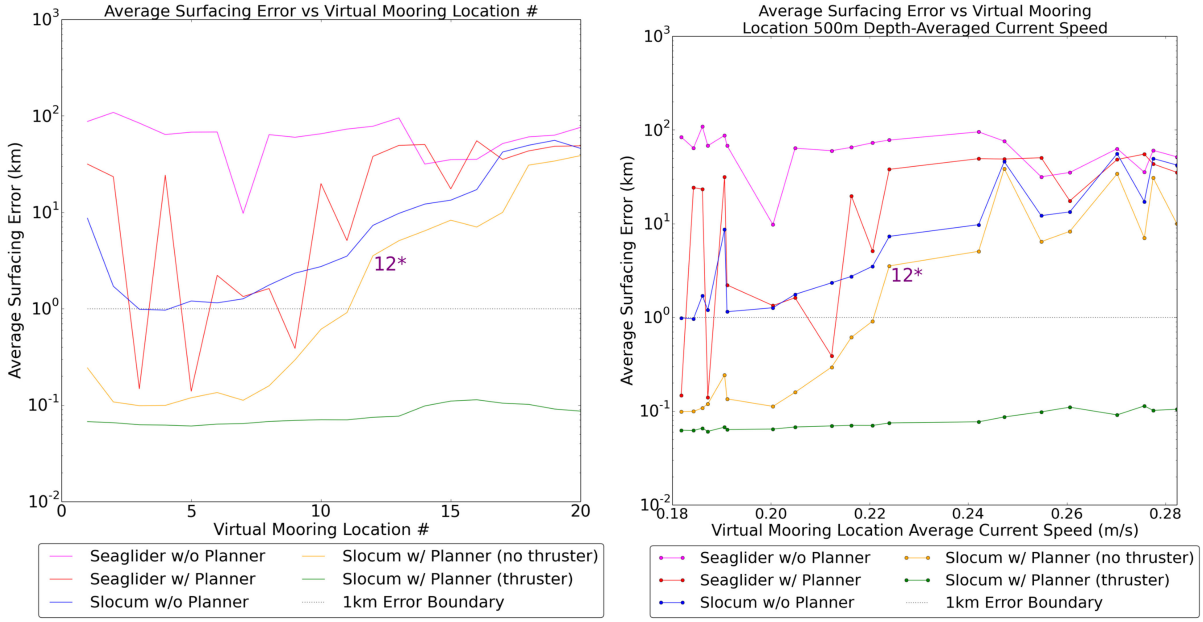

Fig. 13. Average surfacing error for virtual mooring locations on crossover segment 1 for the simulation period July 1, 2017 to September 30, 2017, using planning model = nature model. (Left) Average surfacing error as a function of virtual mooring location number, from south to north. (Right) Average surfacing error as a function of the 500-m depth-averaged current speed at each virtual mooring location. Virtual mooring location 12 is selected for more detailed study as a virtual mooring location where the SWOT station-keeping requirements are achievable using a thruster-equipped Slocum glider, but not without a thruster.

locations. Interestingly, especially for the seaglider with planner, we saw that even a small change in initial conditions (e.g., two adjacent virtual mooring locations separated by 7.5 km) could affect the average surfacing error by up to tens of kilometers. This is most likely explained by the fact that the seagliders are operating in a chaotic system at the edge of their abilities—even a 7.5-km change in initial position could make the difference between staying relatively on target or being swept away into a more challenging current regime, which further dooms any chance for successful station keeping. It should be noted that the results in Fig. 13 represent an upper bound on performance, because the planning model was identical to the nature model.

One worry for vehicles using thrusters is that although their additional control authority may allow them to stay closer to the station-keeping location, they will run out of battery during the deployment and then drift away. The total vehicle energy expenditure over the course of the deployment is given by

$$E = \int_{\text{start}}^{\text{end}} pT(t) + p_N)dt \tag{10}$$

where $p_T(t)$ is the thruster power set point as a function of time and p_N is the nonthruster power usage of the vehicle during normal operation. The nonthruster power usage for a station-keeping G2 Slocum glider was empirically determined to be $p_N = 2.43$ W through field trials. Leaving 10% of the total battery capacity for recovery, the default operational battery capacity of a G2 Slocum glider is approximately 6.55 kW·h, or the battery module can be extended to increase the operational capacity to about 8.87 kW·h. We found that in simulations using the thruster, the Slocum always used more energy than operationally available, from about 9.92 kW·h in the best cast scenario to 10.52 kW·h in the worst, of which 5.25 kW·h was spent on nonthruster functions of the vehicle, and the rest was spent on the thruster. The energy usage could likely be improved by better planning, since the planning algorithm is a greedy algorithm that always prioritizes immediate station-keeping performance over energy usage or long-term station-keeping performance. Additionally, we observe that, because station keeping with less than 1.0 km average error is achievable without thruster usage for many of the virtual mooring locations, in some cases, much of the thruster energy is being spent in a regime where the additional station-keeping performance gains are unnecessary to fulfill the SWOT CalVal requirements. Unfortunately, this is more true at the easier virtual mooring locations and less true at the problematic ones. Nevertheless, the energy usage issues could be improved as a first pass by tuning the thruster set point values available to the planner and the watch circle radius, or more optimally by implementing a more sophisticated planner that plans further ahead and takes energy usage into account in its utility function. Furthermore, the next generation of Slocum gliders will incorporate larger pumps, leading to increased speed from the buoyancy engine, which could mean less necessity for supplementing speed using the thruster. Still, if thrusters are used for Slocums in the final SWOT CalVal virtual mooring configuration, it is likely that the vehicles will require the extended battery capacity modification.

Virtual mooring location 12 on crossover segment 1 represents an interesting opportunity to further study because station keeping under 1.0-km average error was achievable there with use of the thruster but not without it. The next several plots delve more deeply into the reasons for station-keeping failure without use of the thruster. Since we do not have enough *in situ* data near the SWOT crossover C-site to reliably know the nature model RMS error compared to reality, we proceed the investigation with planning model = nature model. It should be remembered that this represents an upper bound on station-keeping performance.

Figs. 14 and 15 show the station-keeping error of the vehicle and the current speed and direction experienced by the vehicle as a function of time throughout its mission for simulation with planning model = nature model. As expected, we can see that the Slocum under planner control with a thruster performs the best station keeping, never even straying across the 1-km error boundary. Under planner control, but without a thruster, the Slocum stays under the 1-km error boundary most of the time, but experiences several discrete periods up to approximately

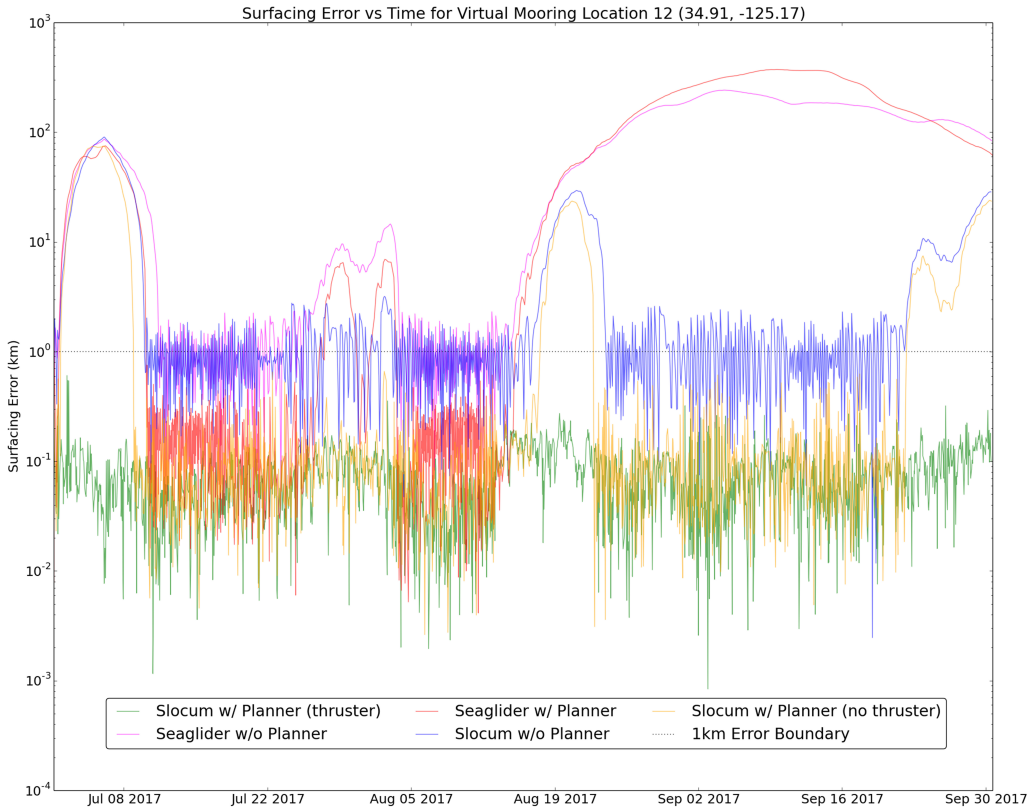

Fig. 14. Surfacing error versus time for crossover 1, virtual mooring location 12, and planning model = nature model.

9 days long where it is blown significantly off course (up to nearly 80 km) before recovering. Observing Fig. 15, we see that these periods are characterized by stronger and more consistently directed currents, with magnitude often greater than the Slocum's maximum through-water speed of 0.35 m/s without thruster assistance. The seaglider fares poorer, spending the majority of the mission tens of kilometers from the station-keeping waypoint, even under planner control.

Overall, we find that precise station keeping is more difficult in locations with stronger and more persistently directed currents. The SWOT crossover C-site provides a much more challenging station-keeping environment than the area near M1, and there is significant variation in station-keeping performance even along a single-crossover segment, suggesting that careful selection of virtual mooring locations will be important for any future virtual-mooring-based SWOT CalVal efforts. We find that the dominant controllable factor in station-keeping performance is the top speed of the station-keeping vehicle, but that an adaptive planner compensating for ocean currents can improve station-keeping performance so long as the currents are not so strong as to make the situation hopeless or so weak as to make the effect of control disturbances due to currents negligible. We show that station keeping under the 1-km average error threshold is possible in simulation for all SWOT crossover segment 1 virtual mooring locations for Slocum gliders equipped with thrusters, and possible for the southern half of the crossover segment for Slocum gliders not equipped with thrusters for the period simulated. Given these results, we believe that a pilot study of the virtual mooring concept using real vehicles at the SWOT Crossover C-site is merited to further develop the concept.

IV. Future Work

The work discussed here could be extended in many directions. First and foremost, more *in situ* deployments would help to establish the applicability of the virtual mooring concept in real-world conditions and provide real data for validating the station-keeping simulation and ocean circulation model results. Specifically, an *in situ* pilot study of the virtual mooring concept at the SWOT crossover C-site is merited, especially because ROMS is less accurate that far from the coast due to lack of available input forcing by permanent sensors (e.g., high-frequency radar surface current data). If possible, within bounds of cost, physical moorings should also be deployed at some of the station-keeping locations to directly compare the data gathered from virtual as opposed to permanent moorings.

Weaknesses in predictive ocean circulation modeling could potentially be addressed by utilizing an ensemble model that includes predictions from other ocean models besides ROMS, for example, HOPS, POM, HYCOM, and MITgcm, and also by assimilating *in situ* data from the virtual moorings back into the model at a faster feedback rate than once a day.

The motion model we used for both seagliders and the Slocum glider is geometry-based and quite simplistic. A better physics-based motion model would improve simulation accuracy.

There are several dive parameters that were assumed or set to be fixed for planning purposes, for example, helix dive radius, box helix dive side length, and thruster watch circle radius. With some changes to the vehicle software, the planner could also be allowed to control buoyancy throw, which would allow it to select from a range of different dive speeds through the water. Allowing the planner to control these additional parameters may improve station-keeping performance.

The assets implementing the virtual moorings were assumed to be homogeneous, evenly spaced, and independent. Further studies should investigate how hybrid formations of heterogeneous assets (e.g., traditional moorings, AUVs with more control authority, virtually profiling floats, ships, and even aerial vehicles) could be coordinated to

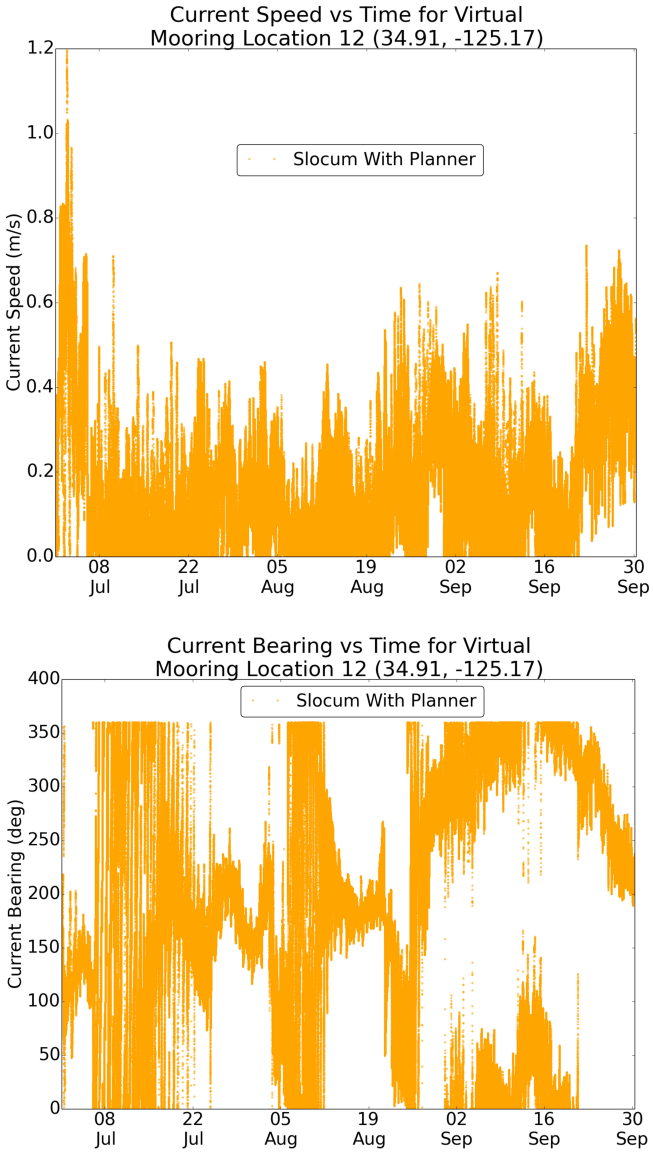

Fig. 15. Asset-experienced current speed (top) and bearing (bottom) versus time for crossover 1, virtual mooring location 12, and planning model = nature model.

create more adaptive and effective observation constellations. To study this, more sophisticated measures of holistic station-keeping performance for the entire constellation should be realized, not just average station-keeping error for individual assets as independent virtual mooring platforms.

The station-keeping planner has much room for improvement. The planning algorithm is greedy and only looks one dive into the future and treats each individual vehicle as independent. In the case of virtual moorings as applied to SWOT CalVal, a more sophisticated planner should be implemented that plans further into the future and optimizes for net data quality collected over the course of the deployment (minimizing SWOT CalVal uncertainty), not just the immediate station-keeping performance on the next dive of one vehicle. This might be particularly relevant in regions where there are strong tidal velocities that may have long periods, but are easy to predict. A more sophisticated planner could also help with energy management for the thrusters, coordinating the virtual mooring array as a coupled observing constellation, or enable more advanced techniques such as forcing all assets to be underwater collecting data at the moment of satellite overflight (instead of transmitting or receiving data on the surface), or biasing the initial starting locations of the virtual moorings based on expected drift over the course of the deployment. The planner could also ingest more sources of information to assist its task. It was assumed that the only information transmitted from the virtual moorings to the planner was the latest surfacing location. Transmission of other information such as sensor measurements tracking vehicle-experienced current velocities or water density could assist the planner in reasoning about the uncertainty in its planning model, and thus inform control recommendations. For example, the planner could model the expected currents for the next dive as some sort of fusion of the currents predicted by the predictive ocean circulation model and the currents measured by the vehicle on recent dives.

The simulation could be used to conduct a much better uncertainty quantification and characterize how various variables affect station-keeping performance, such as current speed, location, time of year, bathymetry, current temporal consistency and spatial distribution, dive frequency, vehicle motion model errors, data transmission latency, and loss of vehicles or duplications of vehicles observing the same location for robustness, among many other possible scenarios.

Even if further study of the virtual mooring concept proves the approach capable of fulfilling the SWOT CalVal requirements in nominal scenarios, SWOT mission planners should conduct a detailed trade study balancing the benefits and risks of the novel failure modalities introduced by the new approach. For example, unlike with a fixed traditional mooring array, an unexpected extreme current event could blow away all gliders during the CalVal period, which could significantly delay CalVal. Likely, in the end, some sort of homogeneous CalVal array using both gliders and traditional moorings could provide a compromise between the benefits of virtual mooring approach and the proven reliability of the traditional mooring approach.

Finally, the virtual mooring concept could easily be adapted to track moving features, as in [34], or maintain more complex formations, as in [4], for example, by moving the target waypoint of each vehicle to follow an oceanic feature or maintain geometry with respect to other vehicles. This could have numerous scientific applications for the oceanographic community, for example, autonomous tracking and sampling of ocean fronts, upwelling, eddies, plankton blooms, icebergs, oil spills, and hydrothermal vent plumes, to name a few.

V. Summary and Conclusion

This paper presents the development and characterization of an adaptive planner using a vehicle motion model and a predictive ocean circulation model to improve station-keeping performance of autonomous underwater gliders in the presence of dynamic ocean currents. We build off of previous underwater glider station-keeping work conducted in [9] and [16], but improve it through the incorporation of predictive current modeling into vehicle control.

A field deployment was conducted in the summer of 2017 to test the planner's performance on real vehicles in a field environment. The field deployment achieved smaller average station-keeping error than the fixed M1 MBARI mooring, and the adaptive planner improved station keeping in situations where the control disturbances due to currents were challenging but surmountable with respect to the station-keeping vehicle's top speed. A simulation framework was developed to investigate the effects of various variables on station-keeping performance that would be difficult to test in the field. To compare the results of the field test to those in simulation, a simulation study was conducted at the same location as the 2017 field deployment and produced usably similar results. Finally, the simulation framework was utilized to study the

viability of using "virtual moorings" implemented with autonomous underwater gliders in place of traditional moorings for calibration and validation of primary instrumentation aboard the upcoming NASA SWOT mission. The study found that unmodified Slocum gliders could fulfill the SWOT station-keeping requirements at about half of the virtual mooring locations, but required a thruster add-on for increased speed for the other half, which would require careful battery management. The study concluded that further investigation into the virtual mooring concept is merited, including a trial field campaign at the SWOT C-site to gather *in situ* data. The methodology developed here could be applied to many oceanic monitoring scenarios: any task where an AUV must stay close to a feature of interest to take measurements, despite the presence of significant control disturbances by currents.

ACKNOWLEDGMENT

Portions of this work were performed at the Jet Propulsion Laboratory, California Institute of Technology, Pasadena, CA, USA, under contract with the National Aeronautics and Space Administration.

REFERENCES

[1] M. A. Moline and O. Schofield, "Remote video assisted docking of untended underwater vehicles," *J. Atmos. Ocean Technol.*, vol. 26, pp. 2665–2672, Dec. 2009.

[2] D. L. Rudnick, "Ocean research enabled by underwater gliders," *Annu. Rev. Mar. Sci.*, vol. 8, pp. 519–541, 2016.

[3] O. Schofield *et al.*, "Maturing glider technology providing a modular platform capable of mapping ecosystems in the ocean," in *Challenges and Innovations in Ocean In-Situ Sensors*, D. A. Pearlman, Ed. New York, NY, USA: Elsevier, 2018.

[4] N. E. Leonard, D. A. Paley, R. E. Davis, D. M. Fratantoni, F. Lekien, and F. Zhang, "Coordinated control of an underwater glider fleet in an adaptive ocean sampling field experiment in Monterey Bay," *J. Field Robot.*, vol. 27, no. 6, pp. 718–740, Nov. 2010.

[5] A. Alvarez, B. Garau, and A. Caiti, "Combining networks of drifting profiling floats and gliders for adaptive sampling of the Ocean," in *Proc. IEEE Int. Conf. Robot. Automat.*, 2007, pp. 157–162.

[6] M. Troesch, S. Chien, Y. Chao, J. Farrara, J. Girton, and J. Dunlap, "Autonomous control of marine floats in the presence of dynamic, uncertain ocean currents," *Robot. Autonom. Syst.*, vol. 108, pp. 100–114, 2018.

[7] Jet Propulsion Laboratory, California Institute of Technology, "Surface water and ocean topography." [Online]. Available: https://www.jpl.nasa.gov/missions/surface-water-and-ocean-topography-swot/. Accessed on: Dec. 13, 2017.

[8] J. Wang *et al.*, "An observing system simulation experiment for the calibration and validation of the surface water and ocean topography sea surface height measurement using in-situ platforms," *J. Atmos. Ocean. Technol.*, vol. 35, pp. 281–297, Feb. 2017.

[9] B. A. Hodges and D. M. Fratantoni, "A thin layer of phytoplankton observed in the Philippine Sea with a synthetic moored array of autonomous gliders," *J. Geophys. Res.*, vol. 114, no. C10, Oct. 2009, Art. no. C10020.

[10] "Iver AUV: New Low Cost AUV for Coastal applications." [Online]. Available: http://www.iver-auv.com/. Accessed on: Dec. 11, 2017.

[11] D. R. Thompson *et al.*, "Spatiotemporal path planning in strong, dynamic, uncertain currents," in *Proc. IEEE Int. Conf. Robot. Automat.*, 2010, pp. 4778–4783.

[12] D. Rao and S. B. Williams, "Large-scale path planning for underwater gliders in ocean currents," in *Proc. Australasian Conf. Robot. Automat.*, 2009, pp. 2–4.

[13] A. A. Pereira, J. Binney, G. A. Hollinger, and G. S. Sukhatme, "Risk-aware path planning for autonomous underwater vehicles using predictive ocean models," *J. Field Robot.*, vol. 30, no. 5, pp. 741–762, Sep. 2013.

[14] K. P. Dahl, D. R. Thompson, D. McLaren, Y. Chao, and S. Chien, "Current-sensitive path planning for an underactuated free-floating ocean Sensorweb," in *Proc. IEEE/RSJ Int. Conf. Intell. Robots Syst.*, 2011, pp. 3140–3146.

[15] D. Jones and G. A. Hollinger, "Planning energy-efficient trajectories in strong disturbances," *IEEE Robot. Automat. Lett.*, vol. 2, no. 4, pp. 2080–2087, Oct. 2017.

[16] D. L. Rudnick, T. M. S. Johnston, and J. T. Sherman, "High-frequency internal waves near the Luzon Strait observed by underwater gliders," *J. Geophys. Res. C, Oceans*, vol. 118, no. 2, pp. 774–784, Feb. 2013.

[17] C. C. Eriksen *et al.*, "Seaglider: A long-range autonomous underwater vehicle for oceanographic research," *IEEE J. Ocean. Eng.*, vol. 26, no. 4, pp. 424–436, Oct. 2001.

[18] D. C. Webb, P. J. Simonetti, and C. P. Jones, "SLOCUM: an underwater glider propelled by environmental energy," *IEEE J. Ocean. Eng.*, vol. 26, no. 4, pp. 447–452, Oct. 2001.

[19] L. Cooney, "Personal communication," Jul. 19, 2018.

[20] J. G. Graver, "Underwater gliders: Dynamics, control and design," Ph.D. dissertation, Dept. Mech. Aerosp. Eng., Princeton Univ., Princeton, NJ, USA, 2005.

[21] B. Claus and R. Bachmayer, "Energy optimal depth control for long range underwater vehicles with applications to a hybrid underwater glider," *Auton. Robots*, vol. 40, no. 7, pp. 1307–1320, Oct. 2016.

[22] P. G. Thomasson and C. A. Woolsey, "Vehicle motion in currents," *IEEE J. Ocean. Eng.*, vol. 38, no. 2, pp. 226–242, Apr. 2013.

[23] J. Sherman, R. E. Davis, W. B. Owens, and J. Valdes, "The autonomous underwater glider 'spray,'" *IEEE J. Ocean. Eng.*, vol. 26, no. 4, pp. 437–446, Oct. 2001.

[24] Y. Chao *et al.*, "Development, implementation and evaluation of a data-assimilative ocean forecasting system off the central California coast," *Deep Sea Res. II, Top. Stud. Oceanogr.*, vol. 56, no. 3, pp. 100–126, Feb. 2009.

[25] A. R. Robinson, "Forecasting and simulating coastal ocean processes and variabilities with the Harvard Ocean Prediction System," in *Proc. Rapid Environ. Assessment, Saclantcen Conf. Proc. Series CP-44,* 1997, pp. 187–198.

[26] G. L. Mellor, "Users guide for a three-dimensional, primitive equation, numerical ocean model," Program Atmos. Ocean. Sci., Princeton Univ., Princeton, NJ, USA, 2003.

[27] E. P. Chassignet, H. E. Hurlburt, and O. M. Smedstad, "The HYCOM (hybrid coordinate ocean model) data assimilative system," *J. Mar. Syst.*, vol. 65, no. 1–4, pp. 60–83, Mar. 2007.

[28] J. Marotzke, R. Giering, K. Q. Zhang, D. Stammer, C. Hill, and T. Lee, "Construction of the adjoint MIT ocean general circulation model and application to Atlantic heat transport sensitivity," *J. Geophys. Res.*, vol. 104, no. C12, pp. 29529–29547, Dec. 1999.

[29] G. Madec, "NEMO ocean engine," Note du Pôle de modélisation, Institut Pierre-Simon Laplace No 27, ISSN No 1288-1619, 2008.

[30] E. Rogers *et al.*, "The NCEP North American mesoscale modeling system: Recent changes and future plans," in *Proc. 23rd Conf. Weather Anal. Forecasting/19th Conf. Numer. Weather Prediction*, 2009, Paper 2A.4.

[31] G. D. Egbert and S. Y. Erofeeva, "Efficient inverse modeling of barotropic ocean tides," *J. Atmos. Ocean. Technol.*, vol. 19, no. 2, pp. 183–204, Feb. 2002.

[32] Y. Chao *et al.*, "Development, implementation, and validation of a California coastal ocean modeling, data assimilation, and forecasting system," *Deep Sea Res. II, Top. Stud. Oceanogr.*, vol. 151, pp. 49–63, May 2018.

[33] M. Durand, L. L. Fu, D. P. Lettenmaier, D. E. Alsdorf, E. Rodriguez, and D. Esteban-Fernandez, "The surface water and ocean topography mission: observing terrestrial surface water and oceanic submesoscale eddies," *Proc. IEEE*, vol. 98, no. 5, pp. 766–779, May 2010.

[34] A. Branch *et al.*, "Front delineation and tracking with multiple underwater vehicles," *J. Field Robot.*, vol. 56, no 3, pp. 62–67, 2018.

Evan B. Clark received the B.S. degree in computer science from Stanford University, Stanford, CA, USA in 2016.

He is currently a Software Engineer with the Artificial Intelligence Group, Jet Propulsion Laboratory (JPL), California Institute of Technology, Pasadena, CA, USA. At JPL, he is engaged on a number of research projects related to marine robotics and autonomy, and is currently in training to become a Curiosity rover driver.

Andrew Branch received the B.S. degree in computer science from Georgia Institute of Technology, Atlanta, GA, USA, in 2015.

He is currently a Software Engineer with the Artificial Intelligence Group, Jet Propulsion Laboratory, California Institute of Technology, Pasadena, CA, USA. His interests focus on autonomous planning and scheduling for space and marine robotic systems.

Steve Chien received the B.S. degree in computer science, minors in economics and mathematics, the M.S. degree in computer science, and Ph.D. degree in computer science from University of Illinois at Urbana-Champaign in 1985, 1987, and 1990, respectively. He is currently Head of the Artificial Intelligence Group and Senior Research Scientist with the Jet Propulsion Laboratory, California Institute of Technology, Pasadena, CA, USA. He has led the deployment of onboard autonomy software to the EO-1, MER, IPEX, and Rosetta missions.

Dr. Chien is a four-time honoree in the NASA Software of the Year competition and was the recipient of four NASA medals for his work in spacecraft autonomy and operations automation.

Faiz Mirza received the B.S. degree in computer science from the University of California—Riverside, Riverside, CA, USA, in 2016, and the M.S. degree in artificial intelligence from the University of Edinburgh, Edinburgh, U.K. in 2017.

He is a Member of Technical Staff in the Artificial Intelligence Group (397I), Planning and Execution Section, of the Jet Propulsion Laboratory, California Institute of Technology, Pasadena, CA, USA. He has previously worked on a combination of RTD efforts and currently working on the extended mission for the ASTERIA CubeSat.

John D. Farrara received the Ph.D. degree in atmospheric sciences from the Department of Atmospheric Sciences, University of California, Los Angeles (UCLA), Los Angeles, CA, USA, in 1989.

His research since then has been centered on numerical modeling of the atmosphere and ocean on regional to global scales. He is currently a Researcher with the Joint Institute for Regional Earth System Science and Engineering, UCLA. His recent work has been concentrated on applications of the Regional Ocean Modeling System in coastal ocean regions.

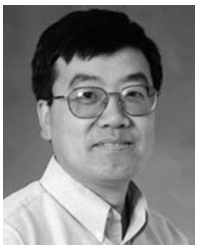

Yi Chao received the Ph.D. degree in oceanography in 1990 from Princeton University, Princeton, NJ, USA, and the Postdoc in 1993 from the University of California, Los Angeles, Los Angeles, CA, USA.

From 1993 to 2011, he was a Scientist with the Jet Propulsion Laboratory, California Institute of Technology, Pasadena, CA, USA. He then founded Seatrec, Inc., Monrovia, CA, USA, where he is currently the CEO. He is also a Scientist with Remote Sensing Solutions, Inc., Barnstable, MA, USA.

David Fratantoni received the Ph.D. degree in physical oceanography from University of Miami in 1996. He is currently an Engineer and Oceanographer interested in ocean circulation, the relationships between physics and biology, and the development of new observational tools and techniques.

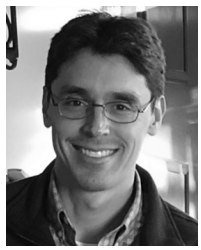

David Aragon received the B.S. degree in electrical engineering from Rutgers University, New Brunswick, NJ, USA in 2005.

He has been operating underwater gliders, coastal radar, and other technologies for more than 10 years for Rutgers Center for Ocean Observing Leadership. Rutgers has maintained a fleet of more than 30 vehicles and an array of coastal radars.

Oscar Schofield received the Ph.D. degree in oceanography form UC Santa Barbara in 1993. He is currently a Distinguished Professor and the Chair of Marine and Coastal Sciences, Rutgers University, New Brunswick, NJ, USA. He is a Co-Founder of Rutgers University's Center for Ocean Observing Leadership that has been deploying ocean observing networks for 25 years. His research interests in the fields of biological oceanography, ocean optics, and new technologies.

Mar M. Flexas received the Ph.D. degree in physical oceanography from Universitat Politécnica de Catalunya, in 2003. She is a Sea-Going Scientist, with experience in the Mediterranean and Antarctic oceanography. She uses *in situ* data, satellite data, laboratory modeling, and numerical techniques to study ocean dynamics, from mesoscale to submesoscale, with particular emphasis on shelf–slope processes and their role in deep ocean ventilation. Since January 2016, she has been at a Senior Research Scientist position with the California Institute of Technology, Pasadena, CA, USA.

Andrew Thompson received the Ph.D. degree in physical oceanography from University of California San Diego in 2006. He is currently a Physical Oceanographer and Professor in environmental science and engineering with the California Institute of Technology, Pasadena, CA, USA. His research combines modeling and observations to study turbulent transport in the ocean and its impact on the large-scale circulation.